Electronic Supplementary Information

Nanoconfinement-induced high-rate performance of hard carbon for densified sodium clusters storage

Experimental Section

Material Synthesis In a typical synthesis process, 2 g of hydroxyl-rich cellulose was ground homogeneously with 10 mg, 20 mg, and 40 mg of carboxyl-rich graphene in mass ratios of 0.5%, 1%, and 2%, respectively, in a mortar and pestle. The sample was then carbonized in a tube furnace under argon atmosphere at a ramp rate of 2 °C per minute at 1300 °C for 2 h. The hard carbon material obtained after carbonization was named HC-G-x (x refers to the percentage of graphene added to cellulose). As a comparison hard carbon (HC) was obtained by carbonizing cellulose under the same conditions, and the obtained hard carbon directly with 1% graphene named as HC@G to verify the graphene orient-induced graphitization.

Electrode Preparation The hard carbon material consisted of a mixture of active material, conductive carbon black (KB) and sodium carboxymethyl cellulose (CMC) in the mass ratio of 90:5:5. The mixed slurry was coated on a copper foil and dried under vacuum at 80°C for 12 h. The mass loading of the active material was 2.8-3.2 mg cm^{-2}. The electrolyte was 1M $NaPF_6$ in DME = 100 Vol% and the separator was glass fiber. All electrochemical tests were performed using CR2032 coin cells and assembled in an argon filled glove box (H_2O < 0.01 ppm, O_2 < 0.01 ppm).

Materials Characterization: The crystal structures of samples are characterized by X-ray diffraction pattern (XRD, D/MAX-Ultima, Japan) with a Cu Kα radiation source and Raman spectroscopy (Raman, Invia Reflex, England). The morphology and microstructure of samples are characterized by SEM (SEM, Regulus 8100, HITACHI) and high-resolution transmission electron microscopy (HRTEM, JEM-F200, Japan). X-ray photoelectron spectroscopy (XPS, ESCALAB 250, USA) is employed to detect the surface valence states of the samples. N_2 adsorption-desorption tests are conducted with Micromeritics ASAP 2460 (USA), the closed pores are investigated using a small angle X-ray scattering system (SAXS, SAXSpoint 5.0).

In/ex-situ measurement: *In-situ* Raman is tested through a customized electrolytic cell device. Na metal is used as the counter and reference electrodes, glass fiber as the separator, and the electrolyte is 1M $NaPF_6$ in DME = 100 Vol%. The in-situ test cell is cycled between 0.01 and 2.0 V. For full cells, $NaNi_{1/3}Fe_{1/3}Mn_{1/3}O_2$ was used as the

cathode, consisting of 90 wt.% active material, 5 wt.% carbon black, and 5 wt.% PVDF coated on aluminum foil, with an anode-to-cathode mass ratio of 1:2~3, with an average N/P ratio of ~1.1. 1,2-dimethoxyethane (DME) and EC/DMC (1:1 v/v) were respectively employed as the electrolytes.

Correlated Calculations

The $d_{(002)}$ value: The average interlayer spacing could be conducted according to Bragg's equation:

$$2d\sin\theta = n\lambda \quad (1)$$

where d is the average interlayer spacing, 2θ is the diffraction angle, λ is the wavelength of the incident X-ray excitation beam, n is the order of reflection.

Diffusion coefficient of sodium ion (D_{Na+}): The diffusion coefficient of sodium-ion (D_{Na+}) can be estimated by the Fick's second law equation: [3]

$$D = \frac{4}{\pi\tau}\left(\frac{m_B V_M}{M_B S}\right)^2\left(\frac{\Delta Es}{\Delta E\tau}\right)^2 \quad (2)$$

in which τ represents the pulse duration, m_B and S are related with the active mass loading and surface area of the electrode, V_M and M_B refer to the molar volume and weight of the active material, ΔEs and $\Delta E\tau$ (refer to voltage variation leaded by galvanostatic charge/discharge and pulse, respectively) can be acquired from the GITT curves.

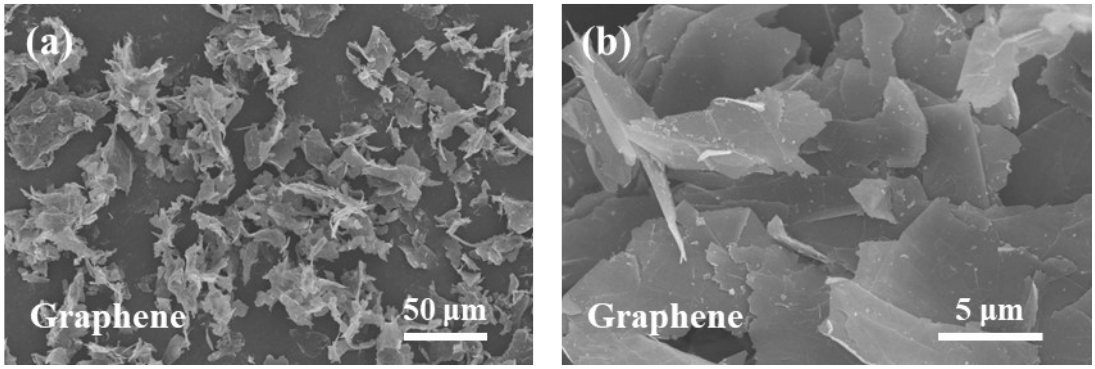

Figure S1. (a-b) SEM images of graphene at different magnifications.

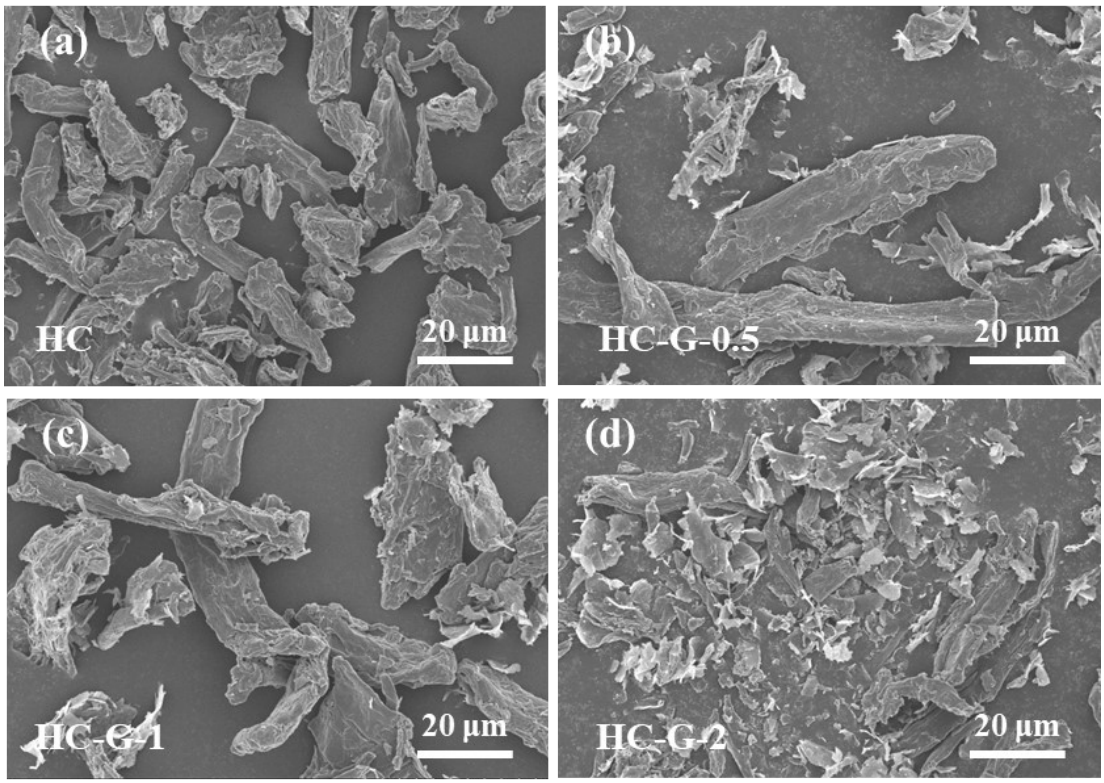

Figure S2. SEM images of (a) HC, (b) HC-G-0.5, (c)HC-G-1, and (d) HC-G-2 samples.

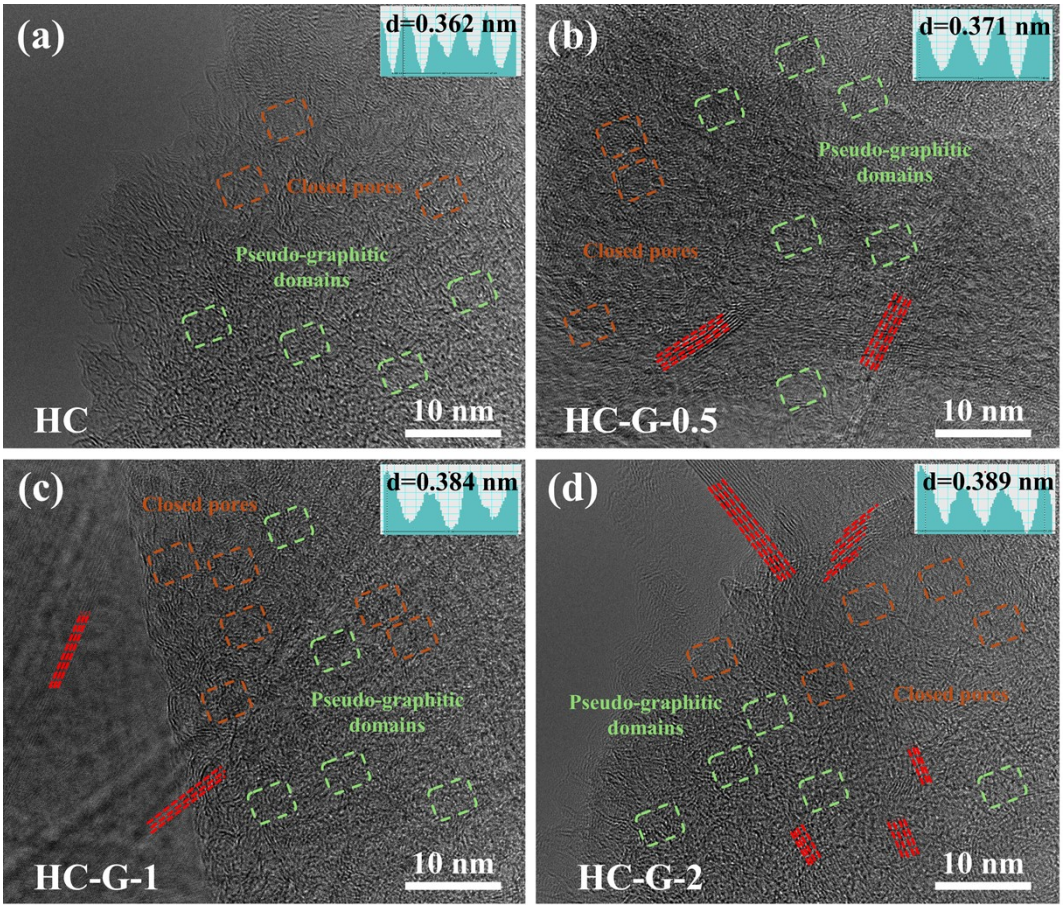

Figure S3. HRTEM images of (a) HC, (b) HC-G-0.5, (c) HC-G-1, and (d) HC-G-2 samples with different pseudo-graphitic domain structures.

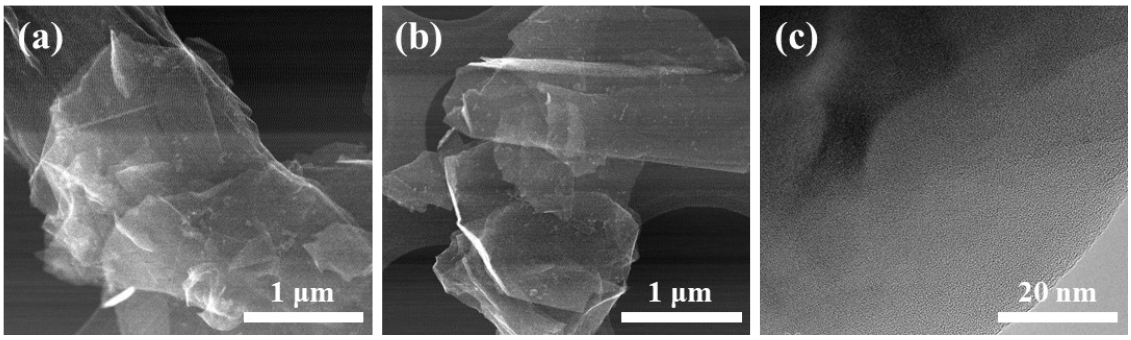

Figure S4. (a-c) The HRTEM images of HC@G with different magnifications, and show the obviously stacked structure.

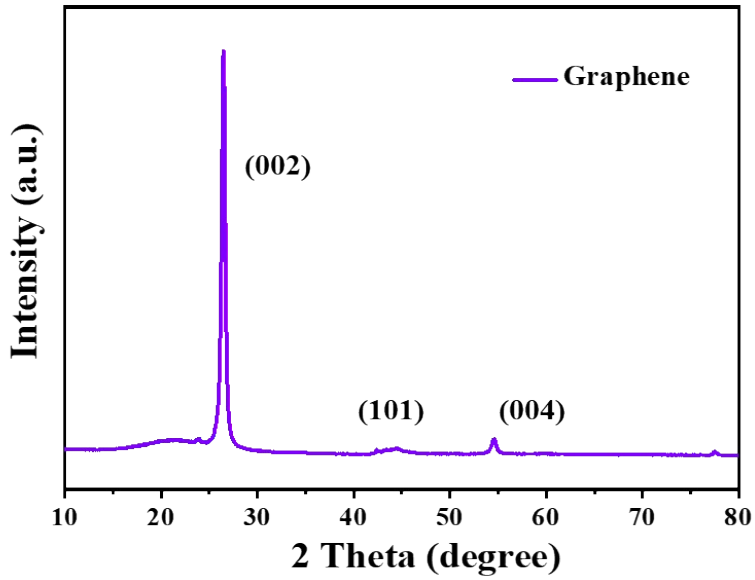

Figure S5. XRD pattern of graphene.

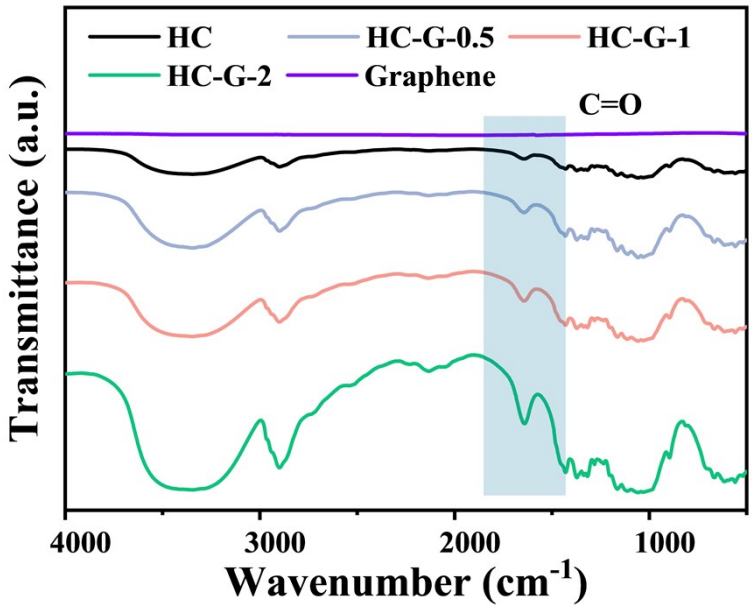

Figure S6. Fourier-transform infrared spectroscopy of the hard carbon precursor from the HC, HC-G-0.5, HC-G-1, HC-G-2, and graphene samples.

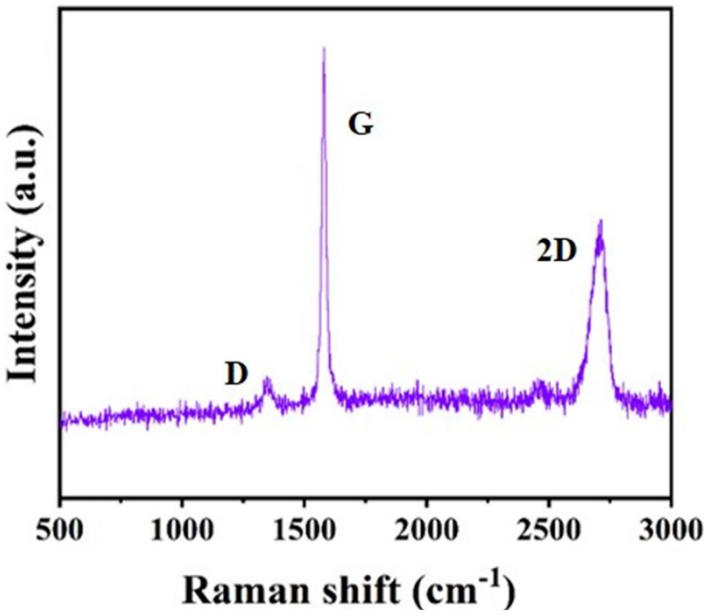

Figure S7. Raman spectral image of graphene.

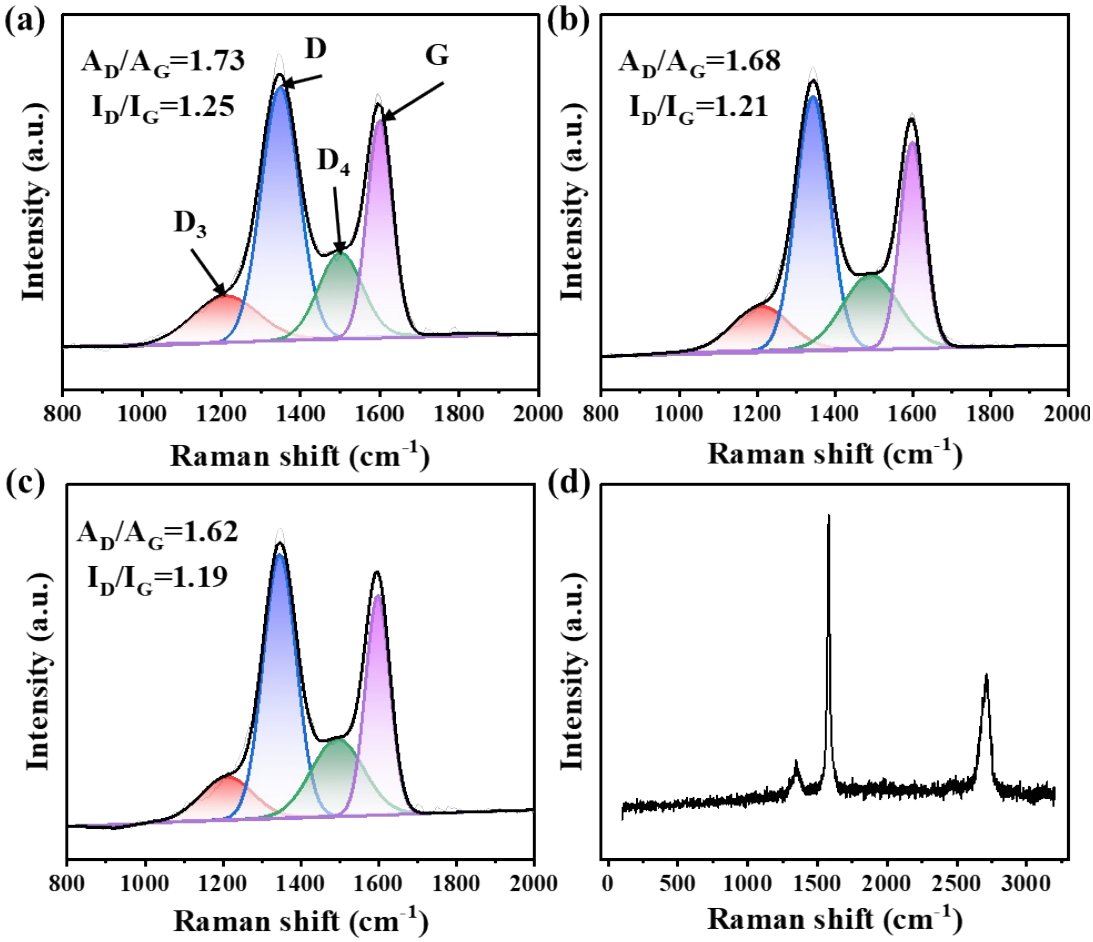

Figure S8. Raman spectra of (a) HC, (b) HC-G-0.5, (c) HC-G-1, (d) HC-G-2 samples.

Text: Based on the common Raman vibrational modes of carbon materials, HC, HC-G-0.5 and HC-G-1 were fitted to four peaks, the D_3 peaks located around 1190-1210 cm^{-1} correspond to sp^2-sp^3 hybridized structures or C-C/C-O stretching vibrations, the D peak located around 1350 cm^{-1} corresponds to a defective sp^2 structure, the D_2 peak located around 1490-1510 cm^{-1} corresponds to amorphous short-range sp^3 carbon defects, the G peak located around 1590 cm^{-1} corresponds to the ordered sp^2 carbon in graphite.

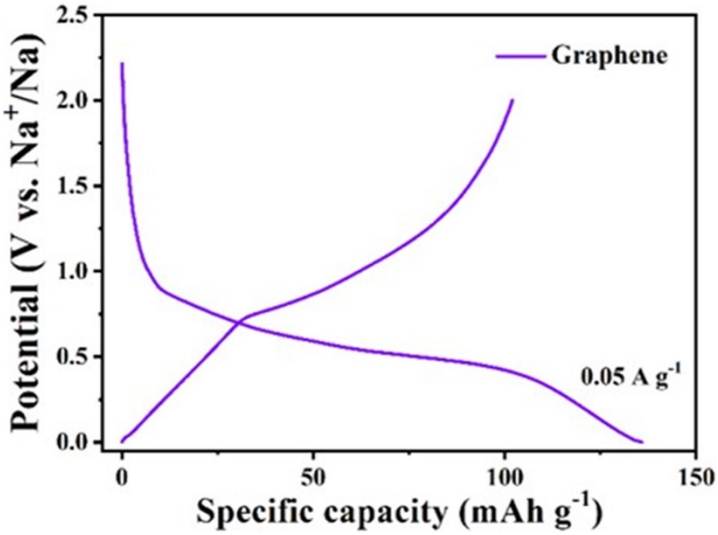

Figure S9. Charge-discharge curves of graphene at a current density of 50 mA g^{-1}.

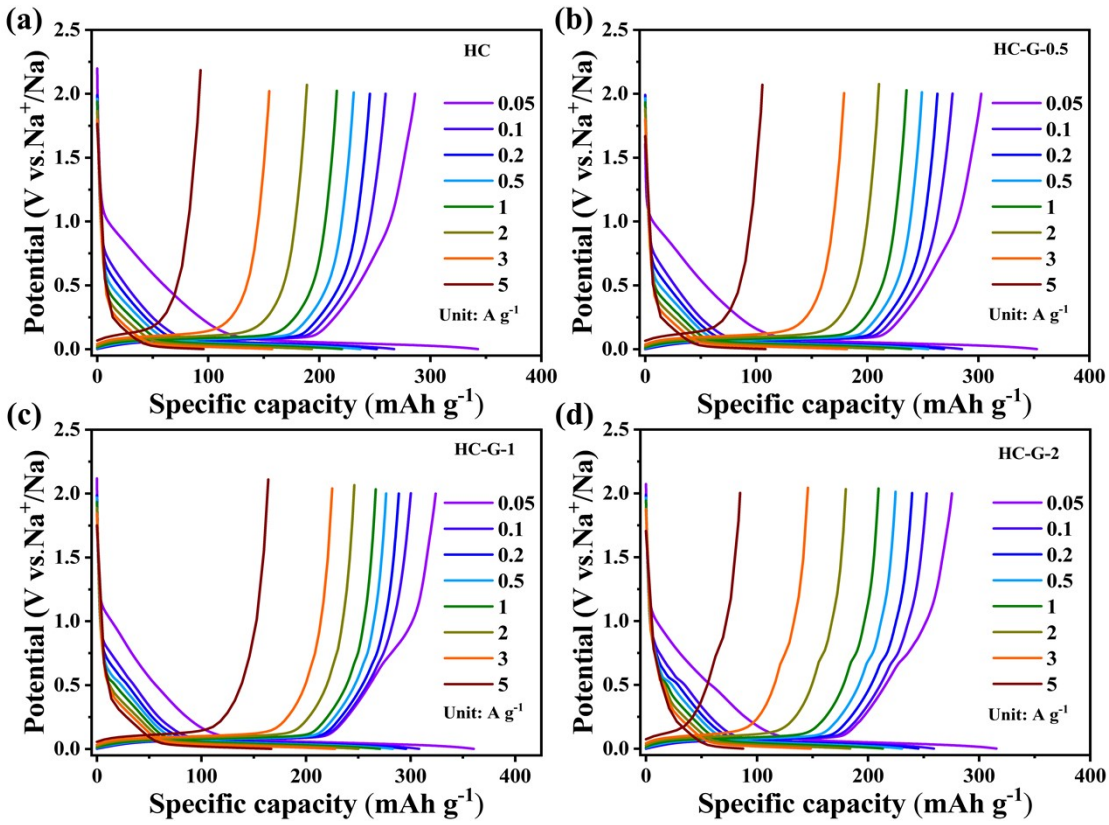

Figure S10. Charge-discharge curves of samples at different current densities. (a) HC, (b) HC-G-0.5, (c) HC-G-1 and (d) HC-G-2 electrodes.

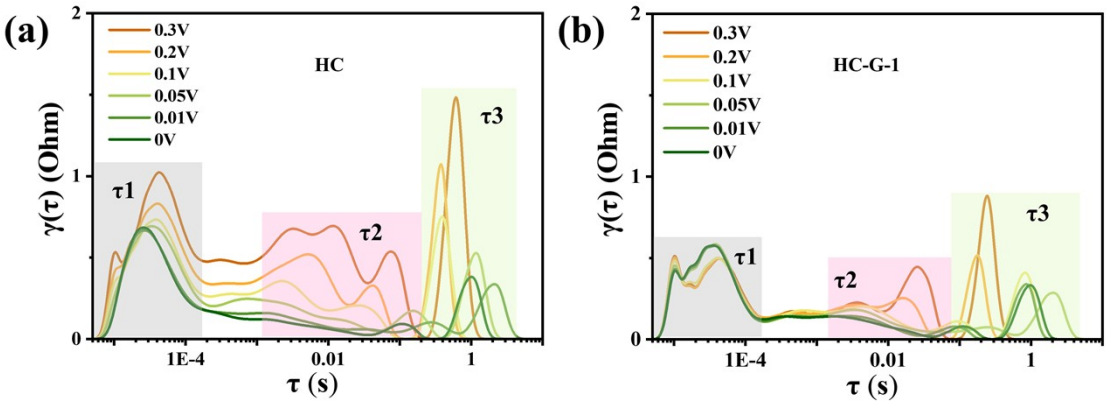

Figure S11. The distribution of relaxation time plots (τ1, τ2, τ3) of HC and HC-G-1 electrodes during the discharging process.

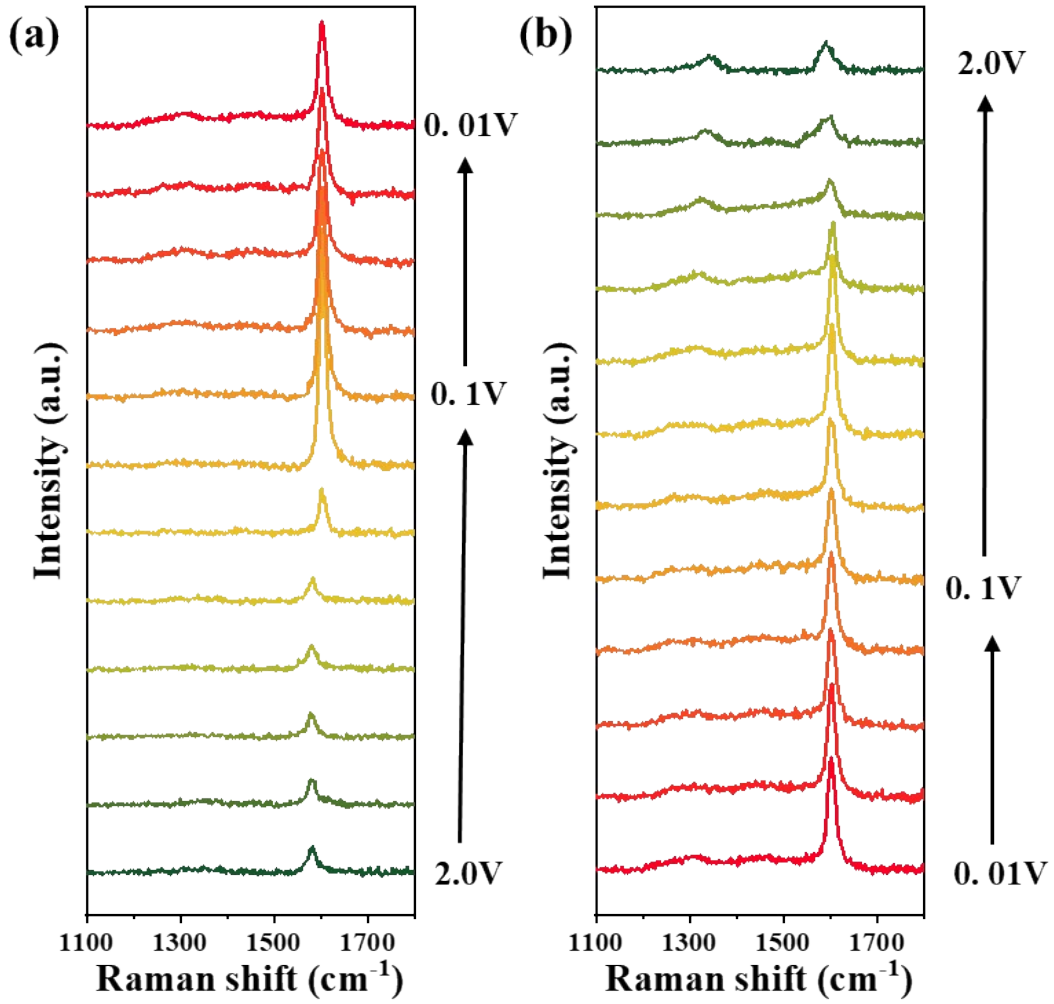

Figure S12. (a-b) *In-situ* Raman spectroscopy of HC-G-1 electrode at discharge from 2 V to 0.01 V, and at charge from 0.01 V to 2 V at a current density of 50 mA g^{-1}.

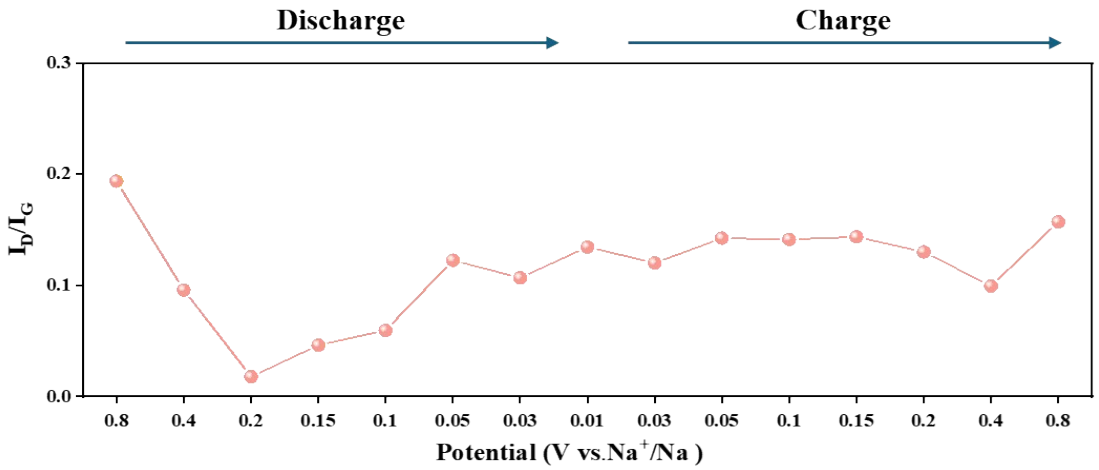

Figure S13. The I_D/I_G ratio at different potential during charge-discharge process of HC-G-1 electrode.

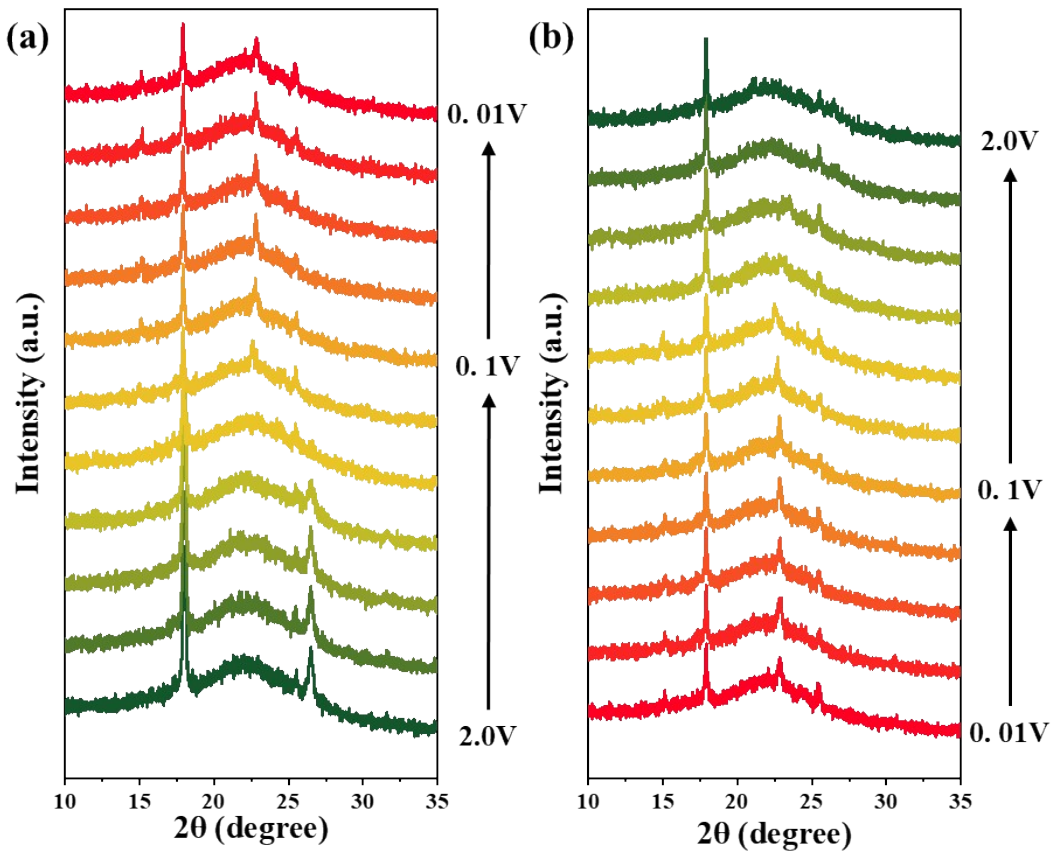

Figure S14. (a-b) *In-situ* XRD patterns of HC-G-1 electrode at discharge from 2 V to 0.01 V, and at charge from 0.01 V to 2 V at a current density of 50 mA g^{-1}.

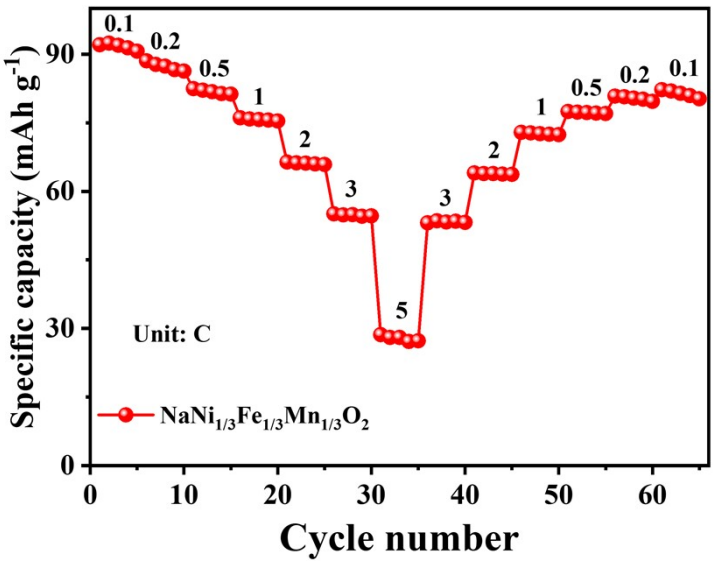

Figure S15. The rate performance of the $NaNi_{1/3}Fe_{1/3}Mn_{1/3}O_2$ cathode.

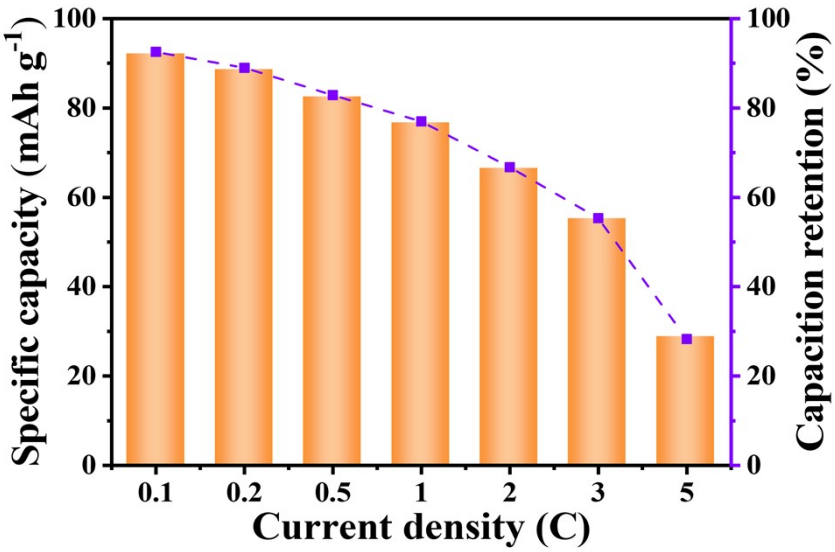

Figure S16. The rate performance of $NaNi_{1/3}Fe_{1/3}Mn_{1/3}O_2$//HC-G-1 full-cell at different current densities (1 C = 300 mA g^{-1}).

Table S1. The interlayer distance (d_{002}), average crystallite width of graphitic domains (L_a), and average thickness of graphitic domains (L_c) from X-ray diffraction (XRD) patterns of the HC, HC-G-0.5, HC-G-1 and HC-G-2 samples.

Samples	d_{002} (nm)	L_a (nm)	L_c (nm)
HC	0.374	11.02	10.55
HC-G-0.5	0.386	10.80	10.48
HC-G-1	0.395	11.09	10.98
HC-G-2	0.398	11.98	11.58

Table S2. Specific surface areas and pore structure calculated from N_2 adsorption/desorption isotherms, and true density and closed pore volume of the HC, HC-G-0.5, HC-G-1 and HC-G-2 samples.

Samples	Specific surface area/ $m^2\ g^{-1}$	Total pore volume/ $cm^3\ g^{-1}$	Average pore size/ nm	True density/ $g\ cm^{-3}$	Closed pore volume/ $cm^3\ g^{-1}$
HC	1.17	0.00808	6.42	2.13	0.0274
HC-G-0.5	3.62	0.00116	8.57	1.97	0.0656
HC-G-1	5.88	0.00198	6.33	1.75	0.129
HC-G-2	421	0.13554	1.85	1.84	0.101